A Letters Journal Exploring the Frontiers of Physics

April 2019

EPL, **126** (2019) 20003 www.epljournal.org
doi: 10.1209/0295-5075/126/20003

# Complexity of energy barriers in mean-field glassy systems

V. Ros[1,2], G. Biroli[1,2] and C. Cammarota[3]

[1] *Institut de physique théorique, Université Paris Saclay, CEA, CNRS - F-91191 Gif-sur-Yvette, France*
[2] *Laboratoire de Physique de l'Ecole normale supérieure, ENS, Université PSL, CNRS, Sorbonne Université, Université Paris-Diderot, Sorbonne Paris Cité - Paris, France*
[3] *King's College London, Department of Mathematics - Strand, London WC2R 2LS, UK*

received 7 January 2019; accepted in final form 23 April 2019
published online 29 May 2019

PACS 05.90.+m – Other topics in statistical physics, thermodynamics, and nonlinear dynamical systems

**Abstract** – We analyze the energy barriers that allow escapes from a given local minimum in a complex high-dimensional landscape. We perform this study by using the Kac-Rice method and computing the typical number of critical points of the energy function at a given distance from the minimum. We analyze their Hessian in terms of random matrix theory and show that for a certain regime of energies and distances critical points are index-one saddles, or transition states, and are associated to barriers. We find that the transition state of lowest energy, important for the activated dynamics at low temperature, is strictly below the "threshold" level above which saddles proliferate. We characterize how the quenched complexity of transition states, important for the activated processes at finite temperature, depends on the energy of the state, the energy of the initial minimum, and the distance between them. The overall picture gained from this study is expected to hold generically for mean-field models of the glass transition.

Copyright © EPLA, 2019

Many complex systems in physics, biology and computer science are characterized by high-dimensional landscapes full of local minima and saddles of any order. Characterizing the statistical properties of critical points in these energy landscapes is instrumental to explain and predict the static and dynamic behavior of such systems [1,2].

Much of the current understanding of this problem comes from the research on the glass transition and on spin-glasses, which played a major role in developing methods to study the generic properties of rough high-dimensional landscapes. Several numerical investigations have introduced ways to map out the network of local minima of the potential energy landscape associated to models of glass-formers, and to characterize their properties [3–8]; whereas theoretical works, started in the 1980s with the development of spin-glass theory [9–12], have obtained the number of critical points and local minima in mean-field models of glasses. Recently, a regain of interest on this subject has come from computer science, and, in particular, machine learning [13] where many central questions concern the statistical properties of rough high-dimensional landscapes originating from the study of the multi-dimensional profile of loss functions. Concomitantly, advances in probability theory and mathematical physics are currently allowing to put the theoretical physics methods on a firmer basis and to obtain new results [14–25].

Despite this great amount of progress on enumerating and classifying local minima, the characterisation of the typical *energy barriers* between them is still to a large extent an open question. The main reason is that, notwithstanding numerical [26–30] and theoretical [12,31–33] attempts in the context of the glass transition, a method to analyze barriers in rough-landscapes is lacking. This is a main obstacle for the development of a theory of dynamics in glassy systems, and in many other contexts where such landscapes play an important role.

Here we show how to solve this major challenge for a central model of rough energy landscapes and of the glass transition [34,35]. Generalizing a method we developed in [24], we work out the full geometrical organization of the typical index-one saddles (heneceforth called *transition states*) that enable escapes from local minima in the spherical $p$-spin model [36]. Our theoretical framework, which builds on the Kac-Rice formula for the computation of stationary points of random functionals [14–20,22], allows us to obtain general results that are expected to hold qualitatively for complex high-dimensional landscapes. From

the mathematical point of view, this represents a first important step towards a full characterization of the Morse complex of random high-dimensional functions.

The energy functional of the spherical $p$-spin model reads

$$E[\mathbf{s}] = -\sum_{\langle i_1,i_2,\ldots,i_p\rangle} J_{i_1,i_2,\ldots,i_p} s_{i_1} s_{i_2} \ldots s_{i_p}, \qquad (1)$$

where the sum runs over all the possible $p$-uplets of indexes $i_k$ (going from 1 to $N$); the configuration $\mathbf{s} = (s_1, \ldots, s_N)$ lives on an $N$-dimensional hypersphere, *i.e.*, $\sum_{i=1}^N s_i^2 = N$, and the quenched random couplings $J_{i_1,i_2,\ldots,i_p}$ are i.i.d. normally distributed random variables with zero mean and variance $\langle J^2\rangle = p!/2N^{p-1}$. At energy density $\epsilon = \lim_{N\to\infty} E[\mathbf{s}]/N$ higher than the ground state, $\epsilon > \epsilon_{\rm gs}$, the model exhibits a number of stationary points which grows exponentially with the dimension $N$. Their stability changes as a function of $\epsilon$ and can be described in terms of the *index*, *i.e.*, the number of downhill directions of the landscape. At high energy the overwhelming majority of critical points are saddles, with an index proportional to $N$. At low energy minima are instead exponentially more frequent than saddles [11,17,37]. The transition between these two regimes is sharp and occurs at a value of the energy density called *threshold*, $\epsilon_{\rm th}(p) \equiv -\sqrt{2(p-1)/p}$, at which typical critical points are characterized by an extensive (in $N$) number of directions with an almost zero curvature. Low-temperature dynamics of the $p$-spin model starting from high-energy initial conditions is essentially a weak-noise dynamical descent in the energy landscape (it becomes a gradient descent in the limit of zero temperature). At small temperatures, penetrating below the threshold and reaching the equilibrium energy requires time scales that grow exponentially with $N$ [38–40]. On these extremely long time scales the system decreases its energy by escaping from local minima via transition states, *i.e.*, *crossing barriers*. This dynamical regime has been studied numerically for some mean-field glassy models in [41–45]. Rigorous results have been obtained for the Random Energy Model [46–48]. In order to develop a theory of activated dynamics in this and more complicated settings, it is crucial to understand how the transition states are organized in configuration space. Pioneering works addressed this problem for mean-field glass systems like the $p$-spin at the end of the 1990s [12,31–33,49]. However the task proved to be so challenging that many central questions remained unanswered. For instance, it is still unknown whether the system has to climb up to the threshold to escape from local minima or can instead sneak through selected paths that involve lower-energy barriers.

Our goal is to address this and similar issues by the quenched Kac-Rice formalism we developed in [24]. Our starting point is the computation of the typical number of saddles surrounding a given minimum. This problem was partially addressed in [12] but in a simpler setting[1]. For convenience, we re-define the state variables setting them on the unit sphere, $\boldsymbol{\sigma} = \mathbf{s}/\sqrt{N}$, and introduce the rescaled energy $h[\boldsymbol{\sigma}] \equiv \sqrt{2/N} E[\sqrt{N}\boldsymbol{\sigma}]$ (see footnote [2]). We denote with $\mathbf{g}[\boldsymbol{\sigma}]$ and $\mathcal{H}[\boldsymbol{\sigma}]$ its gradient vector and Hessian matrix, respectively[3]. We take a fixed minimum $\boldsymbol{\sigma}^0$ drawn at random from the population of minima with energy $\epsilon_0$ ($\epsilon_{\rm gs} \le \epsilon_0 \le \epsilon_{\rm th}$), and define the number $\mathcal{N}_{\boldsymbol{\sigma}^0}(\epsilon, q|\epsilon_0)$ of stationary points with energy $\epsilon$ that are at fixed distance from $\boldsymbol{\sigma}^0$, measured by one minus the overlap $\boldsymbol{\sigma}^0 \cdot \boldsymbol{\sigma} = q$ (high overlap corresponds to small distance). Since saddles above $\epsilon_{\rm th}$ are not the ones used by activated dynamics, we restrict $\epsilon$ to the same range as $\epsilon_0$. $\mathcal{N}_{\boldsymbol{\sigma}^0}(\epsilon, q|\epsilon_0)$ is a random variable, and we are interested in its *typical* value whose logarithm is given by the *quenched* constrained complexity:

$$\Sigma(\epsilon, q|\epsilon_0) = \lim_{N\to\infty} \frac{1}{N} \langle \log \mathcal{N}_{\boldsymbol{\sigma}^0}(\epsilon, q|\epsilon_0)\rangle_0, \qquad (2)$$

where the average is taken over the disorder and the local minima of energy $\epsilon_0$. Its *annealed* counterpart given by $\log\langle \mathcal{N}_{\boldsymbol{\sigma}^0}\rangle_0$ can be used as an approximation and is accessible to rigorous treatments, but it coincides with $\Sigma(\epsilon, q|\epsilon_0)$ in a few cases only [17,19], when the distribution of $\mathcal{N}_{\boldsymbol{\sigma}^0}$ concentrates around its average. The calculation of the quenched complexity follows the method developed recently in [24]; we report below the results and we refer to the Supplemental Material `Supplementarymaterial.pdf` (SM) for their detailed computation and extensions. The quenched complexity reads

$$\Sigma(\epsilon, q|\epsilon_0) = \frac{1}{2}\log\left(\frac{p}{2}(\tilde{z}-\epsilon)^2\right) + \frac{p\big(\epsilon^2 + \epsilon\tilde{z}\big)}{2(p-1)} + \frac{Q}{2}, \qquad (3)$$

where

$$Q = \log\left(\frac{1-q^2}{1-q^{2p-2}}\right) - 2\big(\epsilon_0^2 U_0(q) + \epsilon_0\epsilon U(q) + \epsilon^2 U_1(q)\big),$$

with $\tilde{z} = \sqrt{\epsilon^2 - \epsilon_{\rm th}^2}$ and

$$U_0(q) = \frac{q^{2p}(-q^{2p} + p(q^2-q^4) + q^4)}{q^{4p} - ((p-1)^2(1+q^4) - 2(p-2)pq^2)q^{2p} + q^4},$$

$$U(q) = \frac{2q^{3p}(p(q^2-1)+1) - 2q^{p+4}}{q^{4p} - ((p-1)^2(1+q^4) - 2(p-2)pq^2)q^{2p} + q^4},$$

$$U_1(q) = \frac{q^4 - q^{2p}(p((p-1)q^4 + (3-2p)q^2 + p - 2) + 1)}{q^{4p} - ((p-1)^2(1+q^4) - 2(p-2)pq^2)q^{2p} + q^4}.$$

[1] In [12] the authors compute the number of critical points of the TAP free energy of the spherical $p$-spin model lying at fixed overlap with a given minimum of the free energy; at variance with our calculation, however, their computation is performed within the annealed approximation, and without analysing the structure of the Hessian of the critical points.

[2] Stationary points of (1) with intensive energy $\epsilon$ are also stationary points of the rescaled field with $h[\boldsymbol{\sigma}] = \sqrt{2N}\epsilon$.

[3] Both the gradient vector $\mathbf{g}[\boldsymbol{\sigma}]$ and the Hessian $\mathcal{H}[\boldsymbol{\sigma}]$ are defined taking into account the spherical constraint: $\mathbf{g}[\boldsymbol{\sigma}]$ is an $(N-1)$-dimensional vector which lies on the tangent plane to the sphere at the point $\boldsymbol{\sigma}$. Similarly, $\mathcal{H}[\boldsymbol{\sigma}]$ is an $(N-1)\times(N-1)$ matrix whose matrix elements are given in an arbitrary basis spanning the tangent plane (see the SM for a more precise definition).

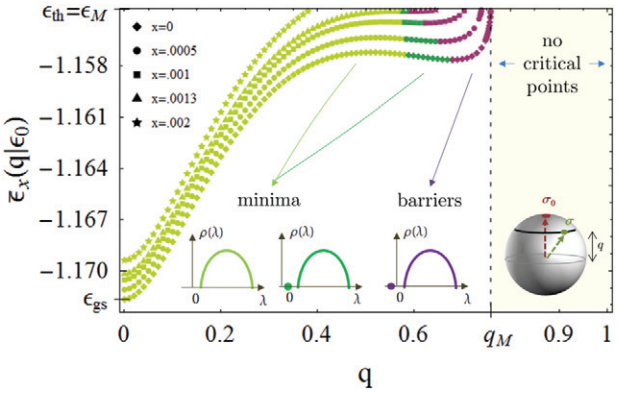


Fig. 1: Energy densities $\overline{\epsilon}_x(q|\epsilon_0)$ of the stationary points at overlap $q$ from the fixed minimum and having complexity $\Sigma = x$, for $p = 3$ and $\epsilon_0 = -1.167 > -1.172 = \epsilon_{\rm gs}$. The green points correspond to minima and the violet points to index-one saddles. The evolution of the density of states of the Hessian is sketched below. Above the threshold energy $\epsilon_{\rm th} = -1.1547$ all points are therefore saddles of index proportional to $N$.

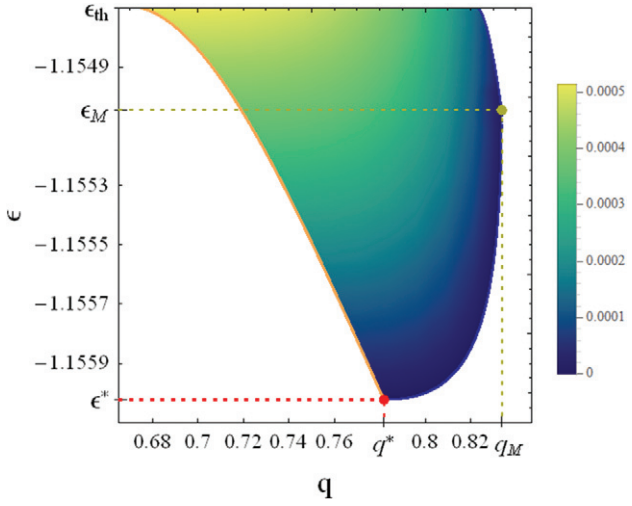


Fig. 2: Complexity of transition states as a function of $q$ and $\epsilon$ for $p = 3$ and $\epsilon_0 = -1.158$. Note that in this case $\epsilon_M < \epsilon_{\rm th}$.

For $q = 0$, one finds $U_0 = U = 0$, $U_1 = 1$, and $Q = -2\epsilon^2$ and we recover the expression of the unconstrained complexity $\Sigma(\epsilon)$ [11], which counts the typical number of stationary points irrespectively of their location in the space of configurations.

The expression (3) for the constrained quenched complexity turns out to be equal to the one of the annealed constrained complexity. This is quite surprising since the presence of the constraint was expected to lead to non-trivial correlations between critical points, and hence to a difference between quenched and annealed averages. It is a fortunate coincidence though, since it simplifies considerably the analysis of the Hessian, and it suggests that a mathematically rigorous proof of (3) along the lines of [19] should be at reach and, moreover, it justifies *a posteriori* the annealed approximation of [12].

We now focus on the properties of the Hessian of the critical points. Depending on the values of $q, \epsilon$ and $\epsilon_0$, we find that as long as $\epsilon < \epsilon_{\rm th}$ the points counted by (3) are either minima or saddles with one unstable direction. More precisely the matrices $\mathcal{H}[\boldsymbol{\sigma}]$ are distributed as $(N-1)\times(N-1)$ GOE matrices with variance $\sigma^2 = p(p-1)$, shifted by a diagonal matrix with entries equal to $\sqrt{2N}p\epsilon$ and perturbed by rank-one matrices that depend on $q, \epsilon$ and $\epsilon_0$. The corresponding bulk eigenvalues density is therefore a shifted semicircle law with a positive support whose lower edge touches zero for $\epsilon \to \epsilon_{\rm th}^-$. Interestingly, the rank-one perturbation can push an isolated eigenvalue out from the semicircle for certain values of parameters (see fig. 1) [50,51]. When this happens, the expression of the isolated eigenvalue reads

$$\lambda_0(q,\epsilon,\epsilon_0) = \frac{\mu(1-\frac{\Delta^2}{2\sigma^2}) + \frac{\Delta^2}{\sigma}\sqrt{\frac{\mu^2}{4\sigma^2} - (1-\frac{\Delta^2}{\sigma^2})}}{(1-\Delta^2/\sigma^2)} - \sqrt{2}p\epsilon, \tag{4}$$

where the expressions of $\mu(q,\epsilon,\epsilon_0)$ and $\Delta^2(q)$ are given in the SM. Its corresponding eigenvector has a finite projection on the direction that points toward $\boldsymbol{\sigma}^0$. Points for which $\lambda_0 < 0$ are saddles having one unstable direction connecting $\boldsymbol{\sigma}$ with $\boldsymbol{\sigma}^0$. Hence, they correspond to possible "mountain-passes" to escape from $\boldsymbol{\sigma}^0$, which we refer to as transition states. In fig. 1 we show iso-complexity energy curves $\overline{\epsilon}_x(q|\epsilon_0)$ defined by $\Sigma(\overline{\epsilon}_x, q|\epsilon_0) = x$ for fixed $\epsilon_0$: $\overline{\epsilon}_x(q|\epsilon_0)$ is the energy of typical stationary points with overlap with the reference minimum equal to $q$ and complexity equal to $x$. The curves shows that at high $q$ the energy landscape is convex. Critical points other than $\boldsymbol{\sigma}^0$ only appear beyond a minimal distance from $\boldsymbol{\sigma}^0$, *i.e.*, $q \leq q_M$. The closest ones at $q_M$ have an energy $\epsilon_M$ that, depending on $\epsilon_0$, is either the threshold energy or it is slightly below it (see fig. 3). They are transition states. Increasing the distance to $\boldsymbol{\sigma}^0$, the isolated eigenvalue grows until it becomes positive, and critical points become minima. On the iso-complexity curves this happens when $\overline{\epsilon}_x(q|\epsilon_0)$ reaches a local minimum (change from purple to green in fig. 1). We do not have any intuitive explanation of this intriguing coincidence, but we recall that the non-monotonic dependence of $\overline{\epsilon}_x(q|\epsilon_0)$ was already noted in [37] for $x = 0$. At even larger distances, the isolated eigenvalue enters into the semi-circle. Eventually, at $q = 0$, we recover the unconstrained complexity result. Among the different curves in fig. 1, the lowest one corresponding to $x = 0$ is of particular interest since it gives the typical energy of the deepest stationary points found at overlap $q$ with $\boldsymbol{\sigma}^0$. Its local minimum at high overlap, which we denote by $(q^*, \epsilon^*)$, gives the lowest energy barrier $\epsilon^* - \epsilon_0$ that can be used to escape from $\boldsymbol{\sigma}^0$.

From this analysis at fixed $\epsilon_0$, two relevant information on the landscape can be deduced: i) there exists a minimal energy barrier that the system has to cross dynamically to exit from the minimum $\boldsymbol{\sigma}^0$. This *optimal barrier*, which

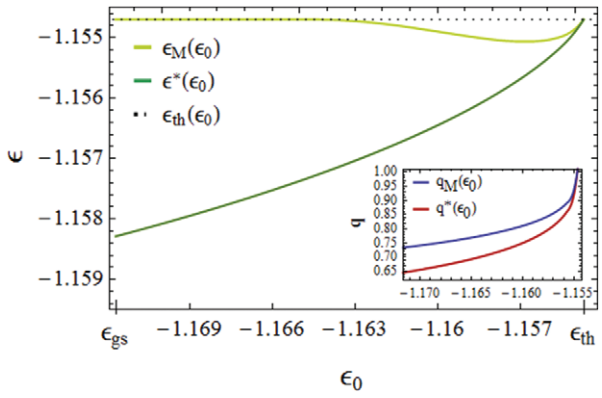


Fig. 3: Energy $\epsilon_M$ of the closest transition states at overlap $q_M$, and energy $\epsilon^*$ of the minimal-energy ones, as a function of $\epsilon_0 \in [\epsilon_{gs}, \epsilon_{th}]$. For $-1.16421 \leq \epsilon_0 \leq \epsilon_{th}$, the closest transition states have energy that is below the threshold (black dotted line). Inset: latitudes $q_M(\epsilon_0)$ of the closest transition states and latitude $q^*(\epsilon_0)$ of the ones of minimal energy.

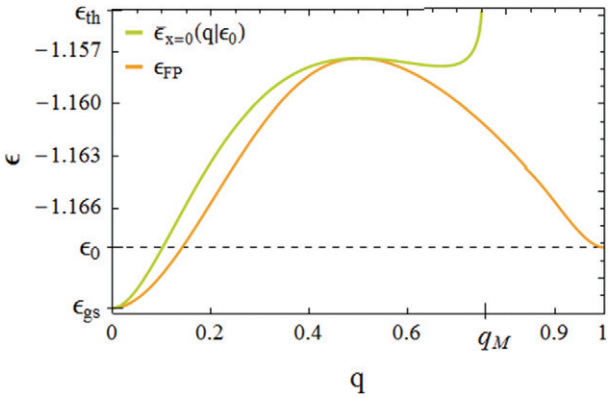


Fig. 4: Comparison between the energy density $\bar{\epsilon}_{x=0}$ of the critical points with $\Sigma = 0$, and the zero-temperature FP potential $\epsilon_{FP}$, for $p = 3$ and $\epsilon_0 = -1.1682$.

is generically lower than $\epsilon_{th} - \epsilon_0$, is the one relevant for activated dynamics at very low temperature[4]; ii) there is an exponential number of transition states corresponding to higher-energy barriers. These are relevant for slow dynamics at finite temperature, where higher but more numerous barriers are favored [1]. Their organization and their complexity is shown in fig. 2. At high $q$, transition states have high energies and low complexity. Note that at the considered $\epsilon_0$, we have $\epsilon_M < \epsilon_{th}$. The spectrum of possible energies is maximal at the $q = q^*$ corresponding to the optimal barriers. It then shrinks to zero at low $q$, in correspondence to the highest and most numerous transition states.

This scenario depends on $\epsilon_0$ in the following way. The energy of the optimal transition states, $\epsilon^*(\epsilon_0)$, remains always below the threshold, and converges to it only when $\epsilon_0 \to \epsilon_{th}^-$, see fig. 3. A plot of the dependence of the optimal barrier $\epsilon^*(\epsilon_0) - \epsilon_0$ is given in the SM. A comparison with [17,37] shows that the energy of these states, despite being below the threshold, is nevertheless much higher than the energy of generic index-one saddles with the same complexity as the minima of energy $\epsilon_0$ (see SM for details). This fact points toward a complex geometrical organization of the critical points in phase space. As shown in fig. 3, the energy $\epsilon_M$ of the closest transition states at $q_M$ also tends to $\epsilon_{th}$ when $\epsilon_0 \to \epsilon_{th}^-$, however it shows a non-monotonic dependence on $\epsilon_0$ (see footnote [5]). In summary, the spectrum of available transition states is larger for smaller $\epsilon_0$ and shrinks when approaching the threshold, where marginal stationary points are expected to be immediately surrounded by other marginal stationary points [12]. This is confirmed in the inset of fig. 3, where the overlap of the closest states, $q_M(\epsilon_0)$, as well as the overlap of the optimal ones $q^*(\epsilon_0)$, are shown to approach one when $\epsilon_0$ reaches $\epsilon_{th}$.

The curve $\bar{\epsilon}_{x=0}(q|\epsilon_0)$, which measures the deepest stationary points at overlap $q$ from $\boldsymbol{\sigma}^0$, shares similarities with the so-called Franz-Parisi (FP) potential [52]. Since we are focusing on the energy landscape, and not the free-energy one, the suitable Franz-Parisi potential to compare with is the one at zero temperature: the minimal energy of configurations at overlap $q$ from $\boldsymbol{\sigma}^0$. We compute it in the SM using standard replica techniques [52] and we compare it to $\bar{\epsilon}_{x=0}(q|\epsilon_0)$ in fig. 4. Since critical points are a subset of all configurations at fixed $q$, the FP potential must be generically lower than or equal to $\bar{\epsilon}_{x=0}(q|\epsilon_0)$. As shown in fig. 4, we find i) that the two functions are equal only at $q = 0$ and at the local maximum of the FP potential, for which the associated critical points are actually *minima* (see fig. 1), and ii) that the FP potential is well below $\bar{\epsilon}_{x=0}(q|\epsilon_0)$ at $q = q^*$. These results show that the FP potential is not directly related to the barriers to escape from $\boldsymbol{\sigma}^0$ (see footnote [6]). In order to detect them, generalized three-replica potentials were introduced and studied dynamically [31–33]. On the basis of our results, we expect that even those constructions are not able to capture optimal transition states (as suggested comparing their typical overlaps[7]). The physical reason is that within the three-replica potential formalism the optimal transition states are atypical and in order to probe them

[4]Note that, as also discussed in the conclusion, the optimal barrier is the first one that is crossed by activated dynamics at low temperature. However, it is not necessarily the one that enables a full escape. This depends on the subsequent barriers to which it is connected to. If these are too high, then it could be more convenient for the system to come back to the minimum and follow an alternative path.

[5]Note that even in the cases when $\epsilon_M < \epsilon_{th}$ one can find barriers with energies up to $\epsilon_{th}$, by focusing on small enough overlaps.

[6]The only information that one can gain from the FP potential is that its local maximum provides a lower bound to the height of the optimal barrier encountered by the system during thermal relaxation, *i.e.*, when the system eventually decorrelates reaching zero overlap with the initial configuration [39,40].

[7]In our case, in which the annealed approximation holds, the mutual overlap between optimal barriers is simply given by the square of the overlap $q$ between the minimum and the optimal barriers. For the three replica potential, where the annealed approximation does not hold, it is instead a more complicated function.

one has to combine it with large deviations techniques as shown in [53].

In conclusion, we have worked out the complex organization of the transition states available to escape from a given minimum in the $p$-spin spherical model, obtaining a scenario that is expected to hold generically for mean-field disordered systems displaying a glass transition. Our results suggest several other important directions to investigate further. First, it would be important to generalize our computation to locate all the index-one saddles connected to the reference minimum, not only when they are typical (as analyzed here) but also when they are subdominant (rare) in comparison with other critical points. Second, it is interesting to know the properties of the minima (other than the original one) to which the saddles we have identified are connected to. This would give additional information on activated dynamical paths, that are formed by a sequence of jumps through optimal transition states and subsequent minima. For instance we have found that the optimal transition state to escape a given minimum is placed at an energy that is smaller than the threshold energy. The next important issue to address is finding out whether the lowest optimal transition state encountered through activated paths leading to thermal relaxation (*i.e.*, connecting minima at zero overlap) is also lower than the threshold. In this context one important question is whether an effective description in terms of trap-like dynamics emerges at long times, as discussed for real systems [5] and found for the random energy model [44–48]. The extension of our work to finite temperature, that necessitates to consider the free-energy landscape, is another interesting direction.

Working out the dynamical theory of activated processes in mean-field glassy systems is arguably one of the most important and challenging problem in glass physics. The generalization of the instantonic solutions of the Martin-Siggia-Rose field theory found in [49,54,55] combined with the knowledge gained in this work on the structure and the organization of energy barriers in configuration space provide a promising starting point for this enterprise.

* * *

We thank G. Ben Arous, A. Cavagna, S. Franz and J. Rocchi for discussions. We are particularly grateful to S. Franz and J. Rocchi for stimulating inputs and for sharing with us their unpublished results [53]. This work was partially funded by the Simons Foundation collaboration Cracking the Glass Problem (No. 454935 to GB).

REFERENCES

[1] Kurchan J., *Six out of equilibrium lectures*, *Les Houches Session XC 2008*, edited by Dauxois T. *et al.* (Oxford University Press) 2010, p. 67.

[2] Biroli G., *Slow relaxations and nonequilibrium dynamics in classical and quantum systems*, *Les Houches Summer School*, Vol. **99** (Oxford University Press) 2016.

[3] Middleton T. F. and Wales D. J., *Phys. Rev. B*, **64** (2001) 024205.

[4] Heuer A., Doliwa B. and Saksaengwijit A., *Phys. Rev. E*, **72** (2005) 021503.

[5] Heuer A. and Doliwa B., *Phys. Rev. E*, **67** (2003) 030501.

[6] Heuer A., *J. Phys.: Condens. Matter*, **20** (2008) 373101.

[7] Sastry S., Debenedetti P. G. and Stillinger F. H., *Nature (London)*, **393** (1998) 554.

[8] Schroder T. B., Sastry S., Dyre J. C. and Glotzer S. C., *J. Chem. Phys.*, **112** (2000) 9834.

[9] Bray A. J. and Moore M. A., *J. Phys. C: Solid State Phys.*, **13** (1980) L469.

[10] Kurchan J., *J. Phys. A*, **24** (1991) 4969.

[11] Crisanti A. and Sommers H. J., *J. Phys. I*, **5** (1995) 805.

[12] Cavagna A., Giardina I. and Parisi G., *J. Phys. A: Math. Gen.*, **30** (1997) 7021.

[13] Mehta P., Bukov M., Wang C. H., Day A. G., Richardson C., Fisher C. K. and Schwab D. J., *A high-bias, low-variance introduction to machine learning for physicists*, to be published in *Phys. Rep.* (arXiv:1803.08823).

[14] Fyodorov Y. V., *Phys. Rev. Lett.*, **92** (2004) 240601.

[15] Bray A. J. and Dean D., *Phys. Rev. Lett.*, **98** (2007) 150201.

[16] Fyodorov Y. V. and Nadal C., *Phys. Rev. Lett.*, **109** (2012) 167203.

[17] Auffinger A., Ben Arous G. and Cerný J., *Commun. Pure Appl. Math.*, **66** (2013) 165.

[18] Wainrib G. and Touboul J., *Phys. Rev. Lett.*, **110** (2013) 118101.

[19] Subag E., *Ann. Probab.*, **45** (2017) 3385 (arXiv: 1504.02251).

[20] Fyodorov Y. V. and Khoruzhenko B., *Proc. Natl. Acad. Sci. U.S.A.*, **113** (2016) 6827.

[21] Fyodorov Y. V., Le Doussal P., Rosso A. and Texier C., *Ann. Phys.*, **397** (2018) 1.

[22] Ben Arous G., Mei S., Montanari A. and Nica M., *The landscape of the spiked tensor model*, arXiv:1712.05424 (2017).

[23] Ipsen J. R. and Forrester P. J., *J. Phys. A: Math. Theor.*, **51** (2018) 474003 (arXiv:1807.05790).

[24] Ros V., Ben Arous G., Biroli G. and Cammarota C., *Phys. Rev. X*, **9** (2019) 011003.

[25] Fan Z., Mei S. and Montanari A., *TAP free energy, spin glasses, and variational inference*, arXiv:1808.07890 (2018).

[26] Angelani L., Di Leonardo R., Ruocco G., Scala A. and Sciortino F., *Phys. Rev. Lett.*, **85** (2000) 5356.

[27] Broderix K., Bhattacharya K. K., Cavagna A., Zippelius A. and Giardina I., *Phys. Rev. Lett.*, **85** (2000) 5360.

[28] Doye J. P. K. and Wales D. J., *J. Chem. Phys.*, **116** (2002) 3777.

[29] Grigera T. S., Cavagna A., Giardina I. and Parisi G., *Phys. Rev. Lett.*, **88** (2002) 055502.

[30] Billoire A., Giomi L. and Marinari E., *Europhys. Lett.*, **71** (2005) 824.

[31] Cavagna A., Giardina I. and Parisi G., *J. Phys. A: Math. Gen.*, **30** (1997) 4449.
[32] Cavagna A., Giardina I. and Parisi G., *Barriers between metastable states in the p-spin spherical model*, arXiv:cond-mat/9702069 (1997).
[33] Barrat A. and Franz S., *J. Phys. A: Math. Gen.*, **31** (1998) L119.
[34] Castellani T. and Cavagna A., *J. Stat. Mech.: Theory Exp.*, **2005** (2005) P05012.
[35] Bouchaud J. P., Cugliandolo L. F., Kurchan J. and Mezard M., *Out of equilibrium dynamics in spin-glasses and other glassy systems*, in *Spin Glasses and Random Fields, Series on Directions in Condensed Matter Physics*, Vol. **12** (World Scientific) 1998, p. 161.
[36] Crisanti A. and Sommers H. J., *Z. Phys. B Condens. Matter*, **87** (1992) 341.
[37] Cavagna A., Giardina I. and Parisi G., *Phys. Rev. B*, **57** (1998) 11251.
[38] Cugliandolo L. and Kurchan J., *Phys. Rev. Lett.*, **71** (1993) 173.
[39] Montanari A. and Semerjian G., *J. Stat. Phys.*, **125** (2006) 23.
[40] Ben Arous G. and Jagannath A., *Commun. Math. Phys.*, **361** (2018) 1 (arXiv:1705.04243).
[41] Crisanti A. and Ritort F., *Europhys. Lett.*, **52** (2000) 640.
[42] Crisanti A. and Ritort F., *Europhys. Lett.*, **51** (2000) 147.
[43] Junier I. and Kurchan J., *J. Phys. A: Math. Gen.*, **37** (2004) 3945.
[44] Baity-Jesi M., Biroli G. and Cammarota C., *J. Stat. Mech.: Theory Exp.*, **2018** (2018) 013301.
[45] Baity-Jesi M., Achard-de Lustrac A. and Biroli G., *Phys. Rev. E*, **98** (2018) 012133 (arXiv:1805.04581).
[46] Ben Arous G., Bovier A. and Gayrard V., *Phys. Rev. Lett.*, **88** (2002) 087201.
[47] Cerný J. and Wassmer T., *Probab. Theory Related Fields*, **167** (2017) 253.
[48] Gayrard V., *Probab. Theory Relat. Fields*, **174** (2019) 501 (arXiv:1602.06081).
[49] Lopatin A. V. and Ioffe L. B., *Phys. Rev. B*, **60** (1999) 6412.
[50] Edwards S. F. and Jones R. C., *J. Phys. A: Math. Gen.*, **9** (1976) 1595.
[51] Baik J., Ben Arous G. and Péché S., *Ann. Probab.*, **33** (2005) 1643.
[52] Franz S. and Parisi G., *J. Phys. I*, **5** (1995) 1401.
[53] Rocchi J. and Franz S., in preparation.
[54] Ioffe L. B. and Sherrington D., *Phys. Rev. B*, **57** (1998) 7666.
[55] Biroli G. and Kurchan J., *Phys. Rev. E*, **64** (2001) 016101.